

Observation of the orbital angular momentum spectrum of a light beam

M. V. Vasnetsov,* J. P. Torres, D. V. Petrov,[†] and Lluís Torner

ICFO—Institut de Ciències Fòniques and Department of Signal Theory and Communications, Universitat Politècnica de Catalunya, 08034 Barcelona, Spain

Received April 28, 2003

We demonstrate an experimental scheme that allows the elucidation of the orbital angular momentum discrete spectrum of an arbitrary light signal. The orbital angular momentum spectrum is represented in a Laguerre–Gaussian mode base, and the spectral components are resolved in the frequency domain by exploiting the Doppler frequency shift that is imparted to rotating light beams. © 2003 Optical Society of America
OCIS codes: 120.3180, 070.6020, 100.2650.

Light beams are known to carry orbital angular momentum (OAM),^{1,2} coming from the spatial distribution of the complex field amplitude (optical vortex).³ The OAM manifests itself, e.g., through the helicoidal wave front structure of the Laguerre–Gaussian (LG) modes. The azimuthal index l of a LG mode, LG_p^l , is the winding number of the helicoid, dictating the phase dependence $\exp(il\varphi + ikz)$ (φ is the azimuthal angle, z is the distance along the beam propagation, and k is the wave number). The OAM can be transferred to particles and can set them into rotation,^{4–6} and photons prepared in quantum states with engineered OAM can be used to encode d -dimensional quantum bits, or qudits, in arbitrary Hilbert dimensions.^{7,8} A crucial tool for the management of the OAM of classical and quantum light is the realization of an experimental scheme for the resolution of the OAM spectral content of arbitrary beams. Several schemes have been suggested to separate particular LG modes.^{9–11} Here we demonstrate a scheme to resolve the OAM spectrum of a classical light beam that is shown to be robust and can be employed for arbitrary complex light distributions.

The resolution of the OAM spectrum of a beam prepared in a coherent superposition of several LG modes becomes possible as a result of the beam rotation. When such a beam is rotated with angular velocity Ω , it acquires a series of sidebands at frequencies $m\Omega$, where m are the azimuthal indices of the LG modes that form the input beam.^{12,13} This is the so-called rotational Doppler frequency shift,^{12,13} which has been observed with microwave radiation passing through a rotating Dove prism.^{14,15} However, a beam passing through a rotating element experiences an unwanted angular precession that makes it difficult to analyze its OAM, especially in the optical domain.^{14,15} Nevertheless, since the rotational Doppler shift depends on only the relative rotation between the light beam and the observer, one can rotate the detector instead. We checked both schemes experimentally. A special rotator carrying the Dove prism was manufactured. In this case we obtained a qualitative detection of the frequency beats, however, with noticeable modulation of the signal because of the angular deviation of the analyzed beam. In contrast, a scheme based on a rotating off-axis aperture was found to be more robust and reliable.

The principle of operation of our LG spectrum analyzer is as follows: There is a linearly polarized signal wave in a superposition of three LG_p^l modes, namely, LG_0^{-1} , LG_0^0 (Gaussian beam), and LG_0^1 with real amplitudes A_{-1} , A_0 , and A_1 , respectively. The amplitude of such a beam can be written as

$$E_s(\rho, \varphi) = \frac{1}{2}[A_{-1}u_0^{-1}(\rho)\exp(-i\varphi) + A_0u_0^0(\rho) + A_1u_0^1(\rho)\exp(i\varphi)] + \text{c.c.}, \quad (1)$$

where ρ is the radial coordinate and $u_p^l(\rho)$ are the radial shapes of the LG_p^l modes. The reference beam $E_r(\rho) = \frac{1}{2}A_r u_0^0(\rho)\exp(i\varphi) + \text{c.c.}$ is frequency shifted with respect to the signal wave (f is a frequency shift and A_r is the amplitude of the reference wave). The field E_s can be experimentally resolved into its LG constituents by measurement of its coaxial interference with the reference beam through a small off-axis aperture, rotating around the beam axis with angular velocity Ω . The light intensity inside the off-axis aperture is written as

$$I(t, \rho_a) = \frac{1}{2} \left\{ I_0 + \sum_{m \neq n} A_m A_n u_0^m(\rho_a) u_0^n(\rho_a) \times \cos[(m-n)\Omega t] + A_r u_0^0(\rho_a) \sum_m A_m u_0^m(\rho_a) \times \cos[(f+m\Omega)t] \right\}, \quad (2)$$

where ρ_a is the radial position of the aperture, I_0 is a constant intensity, and $m, n = -1, 0, 1$ are azimuthal indices of the LG modes that form the signal beam. The light intensity passing through such an aperture is modulated in time, thus featuring the corresponding beats between the modes. The amplitudes of the constituent LG modes are obtained by acquisition of the relative strength of the peaks in the Fourier spectrum. Measurements conducted with different ρ_a provide information about the shape of the mode.

Our experimental scheme is shown in Fig. 1(a). The beam splitter, BS1, splits the output Gaussian beam from the He–Ne laser into two beams. The beam traveling in the signal arm was transformed into a beam containing the superposition of LG modes by a properly designed computer-generated hologram

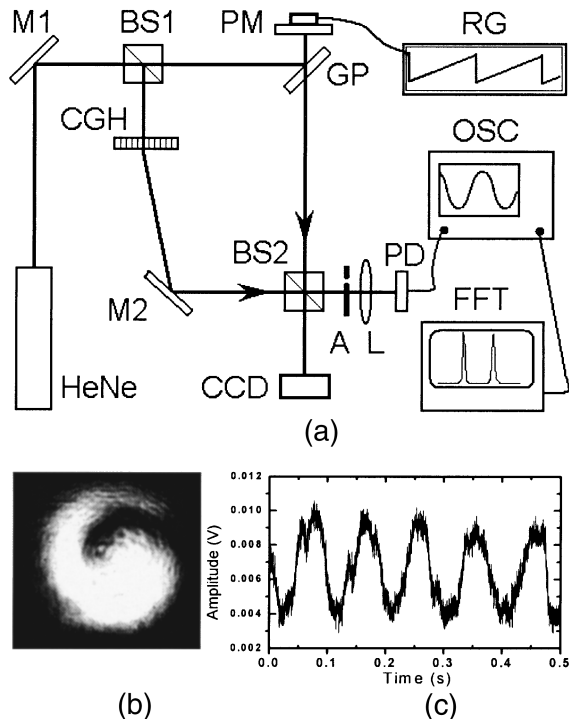


Fig. 1. (a) Experimental setup: M1, M2, mirrors. BS1, BS2, beam splitters; PM, piezo-driven mirror; GP, glass plate. See text for full details and other abbreviations. (b) Spiraling fringe pattern produced by coaxial interference of the LG_0^1 mode and a Gaussian, seen by a CCD camera. (c) Oscilloscope trace of the signal.

(CGH).¹⁶ To get the necessary frequency shift in the reference arm, we used a piezo-driven mirror (PM) with the voltage applied from a ramp generator (RG). The light reflection of $\sim 5\%$ from the glass plate (GP) equalized intensities of the interfering beams. Tuning of the piezo-driven mirror resulted in a linear Doppler frequency shift of approximately $f = 10$ Hz. The second beam splitter (BS2) superposed the signal and reference beams. The continuous rotation of the interference pattern is detected with the aid of the off-axis aperture (A). The beam diameter in the plane of the aperture was measured to be ~ 8 mm. The diameter of the aperture was $300 \mu\text{m}$, and its radial position was 2 mm. The light captured by the aperture was focused into the center of the photodiode (PD) by means of the lens (L). The electric signal was analyzed with the oscilloscope (OSC) with a fast Fourier transform. The off-axis aperture could be set into rotation around the beam axis with a rate of rotation of 100 rpm (angular frequency Ω of ~ 1.67 Hz).

First, we adjusted the experimental scheme to obtain a pure LG_0^1 mode in the signal arm. The coaxial interference of the LG_0^1 mode and the reference wave in the interferometer output produced a spiraling fringe pattern [Fig. 1(b)]. The pattern was analyzed by the off-axis aperture. The oscilloscope trace in Fig. 1(c) demonstrates the rotation of the fringe as a result of the frequency shift in the reference wave. The Fourier spectra of the PD signals acquired in different cases are shown in Figs. 2(a)–2(c). When the off-axis aperture does not rotate, only a peak at $f = 10$ Hz appears [Fig. 2(a)]. When the aperture is set into

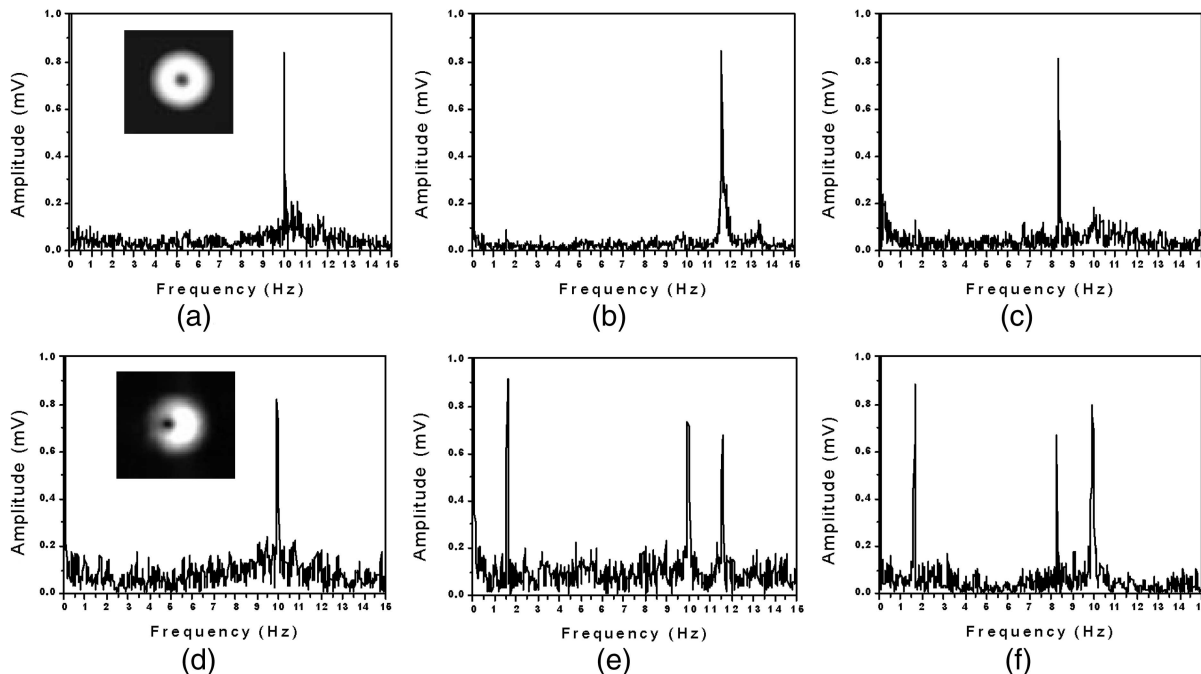


Fig. 2. (a) Spectrum of the signal in Fig. 1(c). The peak at 10 Hz corresponds to the frequency shift f in the reference wave. Inset, LG_0^1 mode. (b) Rotation of the off-axis aperture results in the shift of the peak to the position $f + \Omega \approx 11.7$ Hz. (c) Rotation of the aperture in the opposite direction results in the peak position $f - \Omega \approx 8.3$ Hz. (d) Spectrum of the signal generated by beats between the frequency-shifted reference beam and the superposition of Gaussian and LG_0^1 modes produced by the displaced grating (inset). (e) Rotation of the off-axis aperture results in the new spectral peak at 11.7 Hz and appearance of the peak at 1.7 Hz. (f) Rotation of the aperture in the opposite direction results in the LG_0^1 mode related peak at 8.3 Hz.

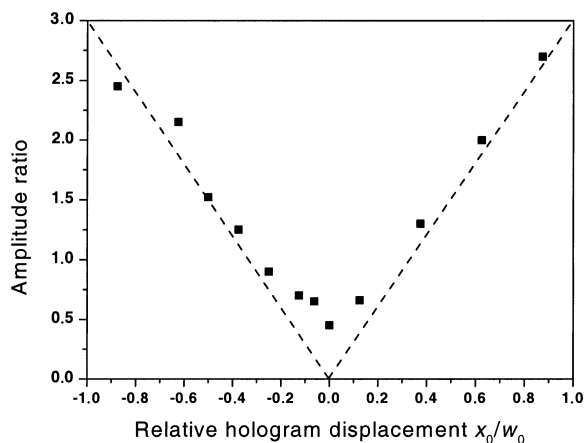


Fig. 3. Ratio of the measured amplitudes of the spectral peaks, corresponding to the LG_0^0 and LG_0^1 components of the signal beam as a function of the hologram relative displacement. The dashed line is a fit to the linear dependence.

rotation, the peak moves to the position $f + \Omega \approx 11.7$ Hz [Fig. 2(b)]. Reversal of the direction of the aperture rotation produces the same effect as an inversion of the azimuthal index from 1 to -1 in the signal wave, namely, the shift of the peak to the position $f - \Omega \approx 8.3$ Hz [Fig. 2(c)].

A light beam comprising a superposition of LG modes was obtained by a small displacement of the hologram relative to the readout beam. Such a displaced hologram produces a combination of LG_0^0 and LG_0^1 modes.^{9,16,17} The Fourier spectra of the signal obtained are shown in Figs. 2(d)–2(f). When no rotation is applied to the off-axis aperture, a single peak observed in the spectrum corresponds to the beats at 10 Hz [Fig. 2(d)]. The rotation of the aperture transforms the spectrum. Two peaks appear at approximately 10 and 11.7 Hz, which correspond to the terms in Eq. (2) oscillating with frequency f and $f + \Omega$. Also, a low-frequency spectral peak appears at 1.7 Hz as a result of the beats between the LG_0^0 and LG_0^1 components of the signal beam [Fig. 2(e)]. Reversing the direction of the aperture rotation changes the position of the LG_0^1 related peak in the spectrum to ~ 8.3 Hz [Fig. 2(f)].

It is important to stress that spectra similar to those discussed above were also obtained in a scheme containing a rotating Dove prism. However, in such case the unwanted beam precession generated pronounced higher harmonics peaks in the measured spectra.

To show that the OAM distribution of a light beam can be continuously varied, and that our scheme allows resolving the corresponding spectrum, we studied the dependence of the spectrum with the displacement of the hologram. An incident Gaussian beam with the center coinciding with the hologram center (on-axis hologram) produces a pure LG_0^1 mode at the output, so no peak at frequency f is present in the spectrum. With the hologram displaced a distance x_0 comparable

with the beam radius w_0 , peaks at both frequencies f and $f + \Omega$ are present. For large values of the displacement, the peak at frequency f dominates. Figure 3 shows the relation between the amplitude of the peaks corresponding to f and $f + \Omega$ as a function of the hologram displacement. The dashed line is the best linear fit of the experimental data, which agrees with the expected linear dependence of the amplitude ratio.¹⁶

In summary, we have demonstrated a scheme that allows the resolution of the OAM spectrum of an optical beam. Such device might be termed an OAM spectrum analyzer. The spectrum is resolved by employing the different rotational Doppler frequency shifts imparted to LG modes with different azimuthal indices.

This work was partially supported by the Spanish Government through grant BFM2002-2861. We thank Alfredo Cano and P. Loza-Alvarez for their help and G. Molina-Terriza for valuable discussions. M. V. Vasnetsov's e-mail address is vasnet@hotmail.com.

*Permanent address, Institute of Physics, National Academy of Science of Ukraine, Kiev, 03039, Ukraine.

†Also with the Institució Catalana de Recerca i Estudis Avançats.

References

1. L. Allen, M. W. Beijersbergen, R. J. C. Spreeuw, and J. P. Woerdman, *Phys. Rev. A* **45**, 8185 (1992).
2. S. M. Barnett, *J. Opt. B Quantum Semiclass. Opt.* **4**, S7 (2002).
3. M. Vasnetsov and K. Staliunas, eds., *Optical Vortices* (Nova Science, Commack, N.Y., 1999).
4. H. He, M. E. J. Friese, N. R. Heckenberg, and H. Rubinsztein-Dunlop, *Phys. Rev. Lett.* **75**, 826 (1995).
5. K. T. Gahagan and G. A. Swartzlander, *Opt. Lett.* **21**, 827 (1996).
6. N. B. Simpson, K. Dholakia, L. Allen, and M. J. Padgett, *Opt. Lett.* **22**, 52 (1997).
7. A. Mair, A. Vaziri, G. Weihs, and A. Zeilinger, *Nature* **412**, 313 (2001).
8. G. Molina-Terriza, J. P. Torres, and L. Torner, *Phys. Rev. Lett.* **88**, 013601 (2002).
9. M. V. Vasnetsov, V. V. Slyusar, and M. S. Soskin, *Quantum Electron.* **31**, 464 (2001).
10. X. Xue, H. Wei, and A. G. Kirk, *Opt. Lett.* **26**, 1746 (2001).
11. J. Leach, M. J. Padgett, S. M. Barnett, S. Franke-Arnold, and J. Courtial, *Phys. Rev. Lett.* **88**, 257901 (2002).
12. G. Nienhuis, *Optics Commun.* **132**, 8 (1996).
13. I. Bialynicki-Birula and Z. Bialynicka-Birula, *Phys. Rev. Lett.* **78**, 2539 (1997).
14. J. Courtial, K. Dholakia, D. A. Robertson, L. Allen, and M. J. Padgett, *Phys. Rev. Lett.* **80**, 3217 (1998).
15. J. Courtial, D. A. Robertson, K. Dholakia, L. Allen, and M. J. Padgett, *Phys. Rev. Lett.* **81**, 4828 (1998).
16. I. V. Basisty, V. V. Slyusar, M. S. Soskin, M. V. Vasnetsov, and A. Ya. Bekshaev, *Opt. Lett.* **28**, 1185 (2003).
17. A. Vaziri, G. Weihs, and A. Zeilinger, *J. Opt. B Quantum Semiclass. Opt.* **4**, S47 (2002).